Microfluidics and Nanofluidics (2022) 26:96
https://doi.org/10.1007/s10404-022-02603-6

RESEARCH PAPER

Surface functionalization of low-cost textile-based microfluidics for manipulation of electrophoretic selectivity of charged analytes

Jawairia Umar Khan[1,4,5] · **Sepidar Sayyar**[1,2] · **Dayong Jin**[5] · **Brett Paull**[3] · **Peter C. Innis**[1,2]

Received: 15 June 2022 / Accepted: 11 October 2022 / Published online: 31 October 2022

Abstract

Textile-based microfluidics offer new opportunities for developing low-cost, open surface-assessable analytical systems for the electrophoretic analysis of complex chemical and biological matrixes. In contrast to electrophoretic fluidic transport in typical chip-based enclosed capillaries where direct access to the sample zone during analysis is a real challenge. Herein, we demonstrate that electrophoretic selectivity could be easily manipulated on these inverted low-cost bespoke textile substrates via a simple surface-functionalization to manipulate, redirect, extract, and characterize charged analytes. This simple approach enables significant improvement in the electrophoretic separation and isotachophoretic (ITP) preconcentration of charged solutes at the surface of open surface-accessible 3D textile constructs. In this work, polyester 3D braided structures have been developed using the conventional braiding technique and used as the electrophoretic substrates, which were modified by dip-coating with polycationic polymers such as chitosan and polyethyleneimine (PEIn). The surface functionalization resulted in the modulation of the electroosmotic flow (EOF) and electrophoretic mobilities of the charged solutes with respect to the unmodified substrates. Chitosan outperformed PEIn in terms of efficient electrophoretic separation and isotachophoretic stacking of an anionic solute. However, PEIn modification resulted in significant suppression of the EOF over a broad range of pH values from 3 to 9 and exhibited fast EOF at acidic pH compared to controlled polyester, which could be promising for the analysis of basic proteins. These findings suggest a great potential for the development of affordable surface-accessible textile-based analytical devices for controlling the specific migration, direction, analysis time, and separation and preconcentration of charged analytes.

✉ Jawairia Umar Khan
jawairia.khan@uts.edu.au

✉ Peter C. Innis
innis@uow.edu.au

1 ARC Centre of Excellence for Electromaterials Science (ACES), AIIM Facility, Innovation Campus, University of Wollongong, Wollongong, NSW 2500, Australia

2 Australian National Fabrication Facility—Materials Node, Innovation Campus, University of Wollongong, Wollongong, NSW 2500, Australia

3 Australian Centre for Research on Separation Science (ACROSS) and ARC Centre of Excellence for Electromaterials. Science (ACES), School of Natural Sciences, University of Tasmania, Hobart, TAS 7005, Australia

4 Department of Fibre and Textile Technology, University of Agriculture, Faisalabad 38000, Pakistan

5 Institute for Biomedical Materials and Devices (IBMD), School of Mathematical and Physical Sciences, Faculty of Science, University of Technology Sydney, Sydney, NSW 2007, Australia

Graphical abstract

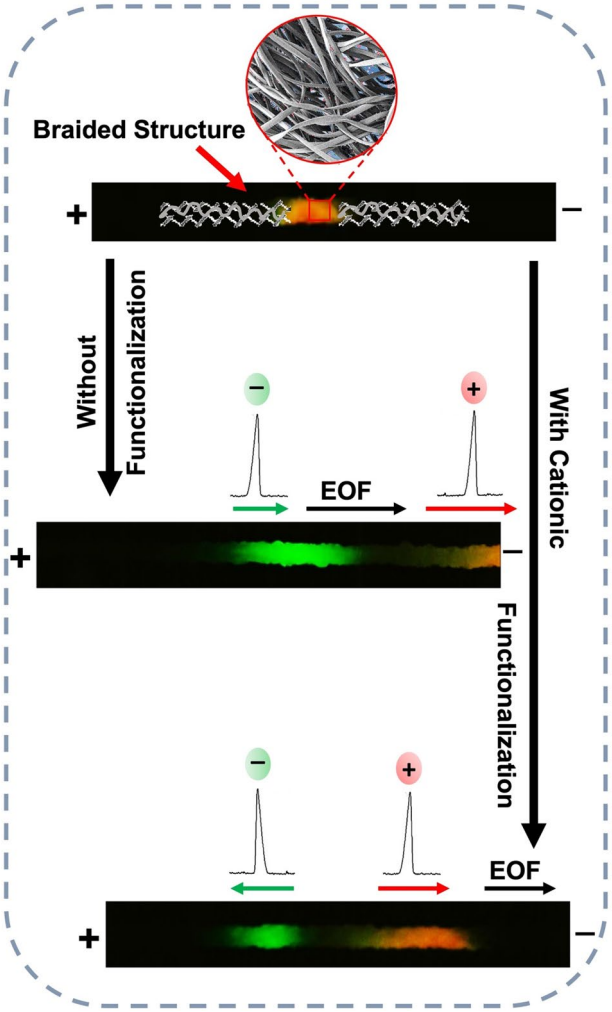

Keywords Textile-based microfluidics · Electrophoresis · Isotachophoresis (ITP) · Surface functionalization · Chitosan · Polyethyleneimine

1 Introduction

Recent developments in microfluidic analytical devices have heightened the need for simple, low-cost, and robust approaches for on-site analysis in medical diagnostics, food safety and environmental monitoring (Whitesides 2006). As a result, microfluidic paper-based analytical devices (μPAD) have emerged as an inexpensive and simple technique for biomedical assays (Martinez et al. 2007). In addition to medical diagnostics (Ratajczak and Stobiecka September 2019), μPADs have been successfully used in applications such as food safety (Weng and Neethirajan 2018) and environmental analysis (Kung et al. 2019). More recently, low-cost textile yarns/threads have been used as a platform for microfluidic diagnostic applications (Reches et al. 2010; Li et al. 2010). Textile yarns are twisted strands of individual textile fibers, which are further combined and twisted to form threads. Yarns provide confined unidirectional fluidic flow through the interfiber micro and nano capillary channels and resulted in a promising alternative for low-cost microfluidic devices. These textile substrates are simple, inexpensive and mechanically strong to be converted into 2D and 3D fabrics using conventional fabrication techniques such as sewing (Xing et al. 2013), weaving (Bhandari et al. 2011), knitting (Narahari et al. 2015), braiding (Khan et al. 2020) and bonding (Baysal et al. 2014). Moreover, the flexible nature of textile materials is an attractive feature not commonly seen in microfluidics devices. Further, the wicking properties of textile fibers that facilitate fluid movement provide the potential for a far simpler approach than the standard

microfluidic chip, which requires external fluid pumping devices for liquid transport (Reches et al. 2010; Li et al. 2010). Unlike μPAD devices, which require hydrophobic barriers patterning to form defined microchannels on the paper substrate, textile substrates promote a unidirectional confined fluid flow resulting from the alignment of the hydrophilic and hydrophobic threads or yarns within the structure via different fabrication techniques such as weaving (Owens et al. 2011). These outstanding characteristics have made the textile-based analytical devices (μTAD) ideal for a diverse range of applications such as point of care diagnostics (Weng et al. 2019), pharmaceuticals (Wei and Lin 2016), food (Guan et al. 2015) and environmental screening (Caetano et al. 2018).

Analyte separation is a primary step for the analysis of complex chemical and biological mixtures. Electrophoretic separation methods, including capillary zone electrophoresis (CZE) and isotachophoresis (ITP), are well known for their outstanding selectivity and high speed of analysis in microfluidics (Ragab and El-Kimary 2019). A fundamental limitation of these approaches is that the capillary channels are typically fully enclosed, affording no direct accessibility to the analyte zone during the separation process, making detection and fractionation more challenging. Alternatively, textile substrates provide an inverted, open and surface assessable platform which has been demonstrated to be capable of supporting electrophoretic separation of charged analytes (Wei and Lin 2016; Wei et al. 2013; Cabot et al. 2016; Xu et al. 2018; Quero et al. 2018). Recently, we reported that simple 3D textile braided structures made of different fibers show significant potential for electrophoretic separation. Here, the braided structure made of polyester yarn was shown to provide an optimal open surface accessible platform as compared to ten different fibers where the analyte moves across the yarn's surface in an inverted manner, in contrasts to enclosed and inherently inaccessible microcapillary format (Khan et al. 2020, 2021). Moreover, sample analytes can be directly micropipetted on the open surface of textile substrate, giving greater flexibility for sample introduction. Additionally, the larger textile surface area, with respect to the conventional microcapillary channels, further alleviates the problem of limiting sample loading capacity due to the small inner surface area of the capillary. A key advantage of the low-cost textile substrate is that the separated analytes can be simply cut from the textile structure and extracted for further analysis on an external detection system (Chen et al. 2020).

Surface modification of inner capillary walls is an important aspect of the CZE and ITP. It has been used to modulate the electroosmotic flow (EOF) for improved separation and through controlling the analyte-surface interactions (Horvath and Dolník 2001). In CZE and ITP, the direction of EOF is normally cathodic (anode to cathode) due to negatively charged surfaces present within fused silica capillaries or PDMS chips. In these systems, the electromigration of anionic analytes is in a counter direction with respect to the EOF (i.e., cathode to anode). Therefore, it is often desirable to suppress or reverse the EOF to achieve a more rapid analysis of the anionic species of interest (Takayanagi and Motomizu 2006). Similarly, during the analysis of cationic species, the strong interaction between the negatively charged silica capillary walls and the positively charged analyte, as in the case of protein analysis, can result in reduced separation efficiency (Stutz 2009). Therefore, several approaches have been developed to modify a capillary's surface charge through covalent modification of the charged surface, physical adsorption of material at the surface, or through modifying the background electrolyte (BGE) by the addition of diffusion-limiting surfactants and polymers to suppress EOF (Hajba and Guttman 2017).

Polycationic reagents such as chitosan (Sun et al. 1994) and polyethyleneimine (PEIn) (Towns and Regnier 1990) are well known for surface modification of silica capillary channels and subsequent reversal of EOF for proteomics. Chitosan (Fu et al. 2007, 2013; Liang et al. 2008) and polyethyleneimine (Córdova et al. 1997; Lucy et al. 2008; Lungu et al. 2016) can be readily adsorbed onto the negatively charged surface present within fused silica capillaries (Sun and Adam Landman 2016) PMMA (Fixe et al. 2004), and PDMS (Liang et al. 2008) chips due to their high density of positive charges in aqueous solution. More recently, cationic surface functionalization has also been reported to improve the performance of paper (Wang et al. 2012) and textile-based (Bagherbaigi et al. 2014; Li et al. 2018) analytical devices. Textile yarns, threads and fabrics can be easily functionalized by a simple surface adsorption dip-coating process akin to textile dying. (Ulum et al. 2016; Erenas et al. 2016; Choi et al. 2018) Polycationic materials such as chitosan and PEIn have been used for the surface modification of textile yarns and threads for a range of applications (Enescu 2008) including the performance enhancement of electrical and electro-thermal properties of graphene-modified smart textiles (Asadi Miankafshe et al. 2019), increasing surface wettability (Li et al. 2018; Walawska et al. 2003), and for the better cell immobilization in biological applications (Bendak and El-Marsafi 1991; Kilonzo et al. 2011; Bech et al. 2007). However, limited applications have been reported in analytical analysis, (Bagherbaigi et al. 2014; Li et al. 2018) and to date, there are no reports of electrophoretic applications using textile-based substrates.

Herein, we hypothesize that following the principle of capillary coatings, the electrophoretic separations on low-cost surface accessible μTAD can be significantly improved. The surface functionalization of textile constructs to modify the surface charge selectively, can potentially alter the EOF and electrophoretic mobilities of the charged analytes to

improve separation efficiency. To investigate this capability, textile structures were selectively functionalized and the modulation of EOF and electrophoretic mobilities of charged solutes on-textile were observed for CZE and ITP processes. 3D textile constructs were fabricated using a conventional braiding technique with commercially available polyester yarn. A simple dip-coating route was adopted for surface functionalization. Chitosan and polyethyleneimine (PEIn) were used to alter the EOF and to investigate its impact on electrophoretic mobility, anionic fluorescein (FL) and zwitterionic rhodamine B (Rh-B) were used as model solutes. The ability to electrophoretically separate the two solutes using ITP focusing was also investigated.

2 Experimental

2.1 Materials and reagents

Polyester yarn (PES) with a linear density of 100 D and 36 filaments was purchased from Shijiazhuang Yunchong Trading Co., Ltd. All chemicals and reagents were of analytical grade and sourced from Sigma Aldrich and used without further modification. Chitosan (75–85% deacetylated chitin, poly(D-glucosamine)) and branched polyethyleneimine (PEIn) (50 wt. % in water, average MW ~ 750,000) were utilized for functionalization and surface modification. Citric acid, sodium citrate dihydrate, glacial acetic acid, sodium acetate, tris-(hydroxymethyl) amino-methane (TRIS), N-cyclohexylamino-2-ethanesulfonic acid (CHES), hydrochloric acid (HCl) and 4-(2-hydroxyethyl)-1-piperazineethanesulfonic acid (HEPES), potassium chloride (KCl), sodium hydroxide (NaOH) were used as electrolytes and for maintaining the pH. Fluorescein sodium salt (FL) and rhodamine B (Rh-B) were used as ionic tracer solutes. Milli-Q grade water (Sartorius Stedim Biotech) was used for all rinsing and solution-making.

2.2 Fabrication and functionalization of 3D structures

Six yarn braided structures were fabricated by mounting the six spools of polyester yarn on alternating positions on a Trenz-Export twelve-head braiding machine, Fig. 1b. Braided structures were precleaned by rinsing with Milli Q water followed by air-drying under the fume hood for 1 h and weighed on a lab-scale weighing machine.

For chitosan treatment, aqueous solutions of 0.25, 0.5, 0.75, 1.0, 1.5, 2.0, 3.0% w/v were prepared by stirring on a hot plate with a magnetic stirrer at 50 °C for 2 h until a clear homogeneous solution was obtained. The solutions were adjusted to pH 3 using acetic acid. For the functionalization of polyester substrates, washed polyester braided structures were dipped in chitosan solutions for half an hour, and coated structures were air-dried overnight at room temperature in a fume hood. Dried structures were rinsed three times with Milli-Q water to remove the unfixed chitosan and to get a neutral pH of 7, which is followed by final drying at room temperature. The weight of coated structures was recorded before and after washing to monitor the percentage add-on of chitosan.

For PEIn functionalization, aqueous solutions of 0.25, 0.5, 1.0, 2.0, and 5.0% (w/v) were prepared and vortex mixed for 30 min. The braided structures were then dipped into the PEIn solution for 2 h and dried in a fume hood overnight. The dried PEIn-coated braids were washed with Milli-Q water three times to obtain a residual pH of 7 and then subsequently dried at room temperature.

2.3 Characterization

The characterization of the surface-modified polyester braids was performed by monitoring the weight change, scanning electron microscopy (SEM) (JEOL JSM 7500-FA), and ATR—FTIR spectroscopy (Shimadzu IRPrestige-21). The surface zeta-potential (ζ) of the controlled, chitosan—functionalized and PEIn-functionalized polyester braids was determined at three different pH values of 3, 5, and 8 using an Anton Paar SurPASS Electrokinetic Analyzer (Australian National Fabrication Facility—Queensland). Fiber plugs of approximately 300–400 mg were formed from the braided structures and placed into the instrument's cylindrical cell accessory. 1 mM KCl solution was used as an electrolyte for the ζ-potential measurements, and the pH was adjusted with NaOH or HCl. Four replicates were taken for each sample.

2.4 Electrophoresis protocols and EOF Measurement

For electrophoresis, 3D printed reservoirs were designed and developed in-house using Solidworks CAD software and Form-2 3D printer. The reservoir design includes a basin for the electrolyte solution, a holder to guide the braid channel, driving electrode mounts and screws to fix the braid channel between two reservoirs. The braided structure was pre-soaked with BGE before being connected between two buffer reservoirs while keeping the channel length as 3.6 cm, as presented in a snapshot in Fig. 1c–e. These two reservoirs were used as inlet and outlet chambers and the textile braided structure was used as the reaction chamber or microfluidic channels. Both reservoirs were filled with BGE,

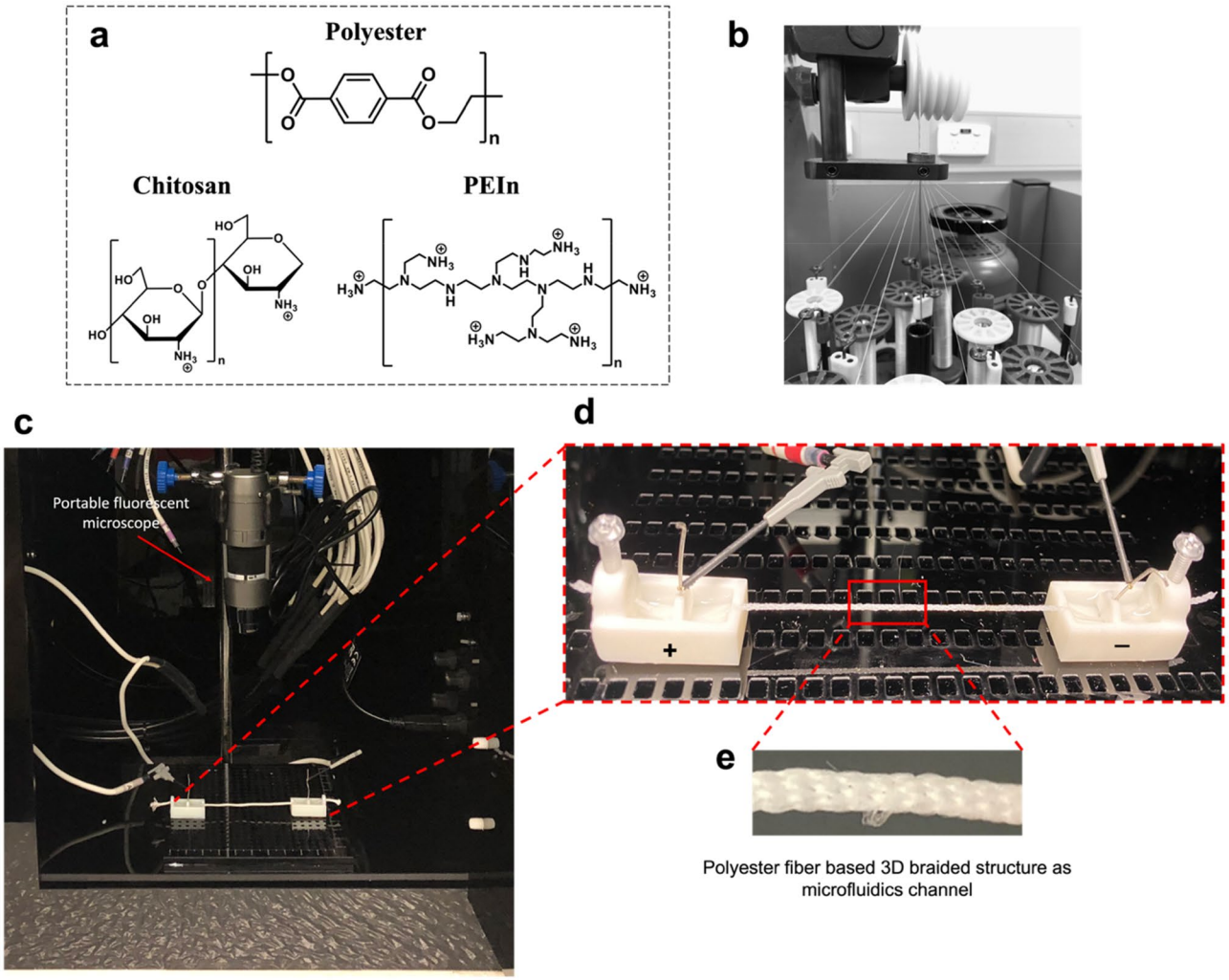

Fig. 1 Fabrication, and experimental setup for electrophoresis. **a** Chemical structures of polyester, chitosan and polyethyleneimine. **b** Snapshot of the braiding machine used for the fabrication of braided structures using the polyester yarn. **c** Snapshot of the textile-based electrophoresis system set-up. **d** Inset showing the braided structure connecting the 3D printed buffer reservoirs and platinum electrodes connected with the power supply. **e** Inset showing the optical microscopic image of the polyester yarn braided structure used as a 3D textile—based multicapillaries channel for electrophoresis

and the system was left for a few seconds to establish equilibrium. A constant DC voltage was applied to driving electrodes using a high voltage sequencer from LabSmith, Inc. (HVS 448LC 3000D) to establish EOF at the fiber surface.

The EOF on the textile structures was monitored using the current monitoring method (Huang et al. 1988). First, the two reservoirs were filled with 2.5 mM TRIS/CHES (pH 8) BGE, and a constant electric field of 100 Vcm^{-1} was applied across the braided structure connected between two buffer reservoirs until a constant current was achieved. Later, the BGE solution in the inlet reservoir was replaced with the BGE of the same composition with a slightly higher concentration (3 mM). Then, a constant electric field was applied between the buffer reservoirs while monitoring the electric current. With the increase in conductivity of the BGE, a gradual increase in current was observed, which stabilizes when the 3 mM BGE replaces the 2.5 mM BGE in the whole length of the braid channel. The EOF mobility μ_{EOF} ($cm^2\ V^{-1}\ s^{-1}$) was calculated by recording the time t (s) taken for current stabilization while 3 mM BGE replaced the 2.5 mM BGE through the full channel length upon applied voltage V (V), Eq. 1. The same procedure was repeated for EOF measurement with acetate buffer (pH 5) and citrate buffer (pH 3), and with braided structures treated with the different polycationic polymers such as chitosan and PEIn solutions.

$$\mathrm{EOF} = \frac{l^2}{Vt} \tag{1}$$

2.5 Electrophoretic separation and isotachophoresis (ITP) protocols

Electrophoretic separation was performed on 3.6 cm long polyester braided structures with and without surface modification. For separation, an analyte mixture was prepared using FL and Rh-B in a molar concentration of 70 µM and 4 mM, respectively. The separation mixture was prepared in 2.5 mM TRIS/CHES BGE solutions to observe the effect of coating on electrophoretic separation at pH 8. A 0.5 µL of sample mixture was micropipetted on the unmodified polyester braided structure as control at 1 cm distance from the anodic reservoir and a voltage of 360 V was applied to initiate the electrophoretic separation. Separation resolution (SR) of the two fluorescent solutes was calculated by determining the quotient of the distance between two adjacent intensity peaks ΔL and the average width W of the fitted peak intensities, Eq. 2. Details of the SR measurement are provided in supporting information S2. The same protocol was repeated for chitosan and PEIn functionalized polyester braids.

$$\mathrm{SR} = \frac{\Delta L}{W} \tag{2}$$

ITP was conducted on unmodified polyester braids as control and on chitosan and PEIn functionalized polyester braided structures. Leading electrolyte (LE) was prepared using 2.5 mM of TRIS buffer titrated with 100 mM HCl at pH 8 and conductivity 124 μScm^{-1}. For trailing electrolyte (TE), 2.5 mM of TRIS buffer titrated with 25 mM of HEPES at pH 7.7 and conductivity 85 μScm^{-1}. FL/Rh-B sample mixture was prepared in TE in a molar ratio of 70 µM: 4 mM, respectively. The polyester braided structure was first soaked in LE to ensure all the micro-capillaries and fiber voids within the braided structure were filled with TE. For ITP, a LE-wetted braid was mounted in the electrophoresis setup between two reservoirs, and anodic reservoir and cathodic reservoirs were filled with LE and TE, respectively. Afterward, a 0.5 µL aliquot of sample mixture was applied using a micropipette onto the braid channel at a position 1 cm from the cathodic reservoir. A constant current of 20 µA was then applied between the two reservoirs, and ITP separation and focusing of FL were observed. The same procedure was repeated with each of the chitosan and PEIn-coated polyester braids.

2.6 Data acquisition

A Dino-Lite fluorescence imaging digital microscope AM4113T-GFBW (blue light excitation LED and 510 nm emission filter) was used to record the fluorescent images and videos at a 30 fps frame rate, Fig. 1c. ImageJ (NIH) and in-house written MATLAB code were used to process the recorded videos. All fluorescent images were background-corrected before further analysis. Origin Pro (Origin Lab Co.) was used for data analysis.

3 Results and discussions

3.1 Cationic-functionalization on polyester braid

The polycationic chitosan (Fig. 1a) can be adsorbed on the negatively charged surface of PES fiber under acidic conditions by simple dip-coating without any fabric pretreatment (Walawska et al. 2003). Different concentrations of chitosan were applied to the PES braided structures to investigate the effect of chitosan—functionalized fiber surface on the electrophoretic mobility of charged analytes. The treated structures were first characterized by weight-change analysis, SEM analysis, FTIR, and then analysed for EOF modification. Similarly, branched PEIn (Fig. 1a) is a highly cationic polymer over a broad pH range (pKa 4.3, 6.4, 9.5) (Jun et al. 2015) with primary, secondary and tertiary amines in a 1:2:1 ratio (Córdova et al. 1997; Lucy et al. 2008). PEIn has been used for both fixed/bonded (Bush et al. 2016) and dynamic coatings (Boonyakong and Tucker 2009) in conventional capillary channels to manipulate EOF and facilitate faster analysis, especially for basic proteins and peptides. PEIn has also been reported for the surface modification of textile fibers for better cell immobilization and other bioprocesses. (Kilonzo et al. 2011) Different PEIn concentrations were applied to the polyester braided structure and analyzed in terms of changes in EOF, electrophoretic separation, and ITP.

The chitosan content on the polyester braid after chitosan coating was almost linear with the increase in chitosan concentration until a plateau is observed after 2% chitosan concentration, Fig. 2a. However, as shown in Fig. 2b, no significant mass gain was observed after dip-coating the polyester braids with the PEIn solutions (details of weight change are provided in supporting information S1). Contrasting the chitosan functionalization, a slight decrease in weight of the braided structure was observed, which is ascribed to the degradative aminolysis of the polyester fibers with PEIn modification. The reaction of the amine group in the PEIn with the ester group of polyester fiber likely led to chain scission that resulted in a weight loss of the polyester fibers as shown by the equation in Fig. 2c (Bendak and El-Marsafi 1991).

The surface morphology of the braided structures was analyzed by SEM before and after chitosan and PEIn-functionalization, Fig. 3a–c. The untreated polyester braid (control sample) presented a clean and smooth longitudinal fibril structure, as shown in Fig. 3a. However, after coating with

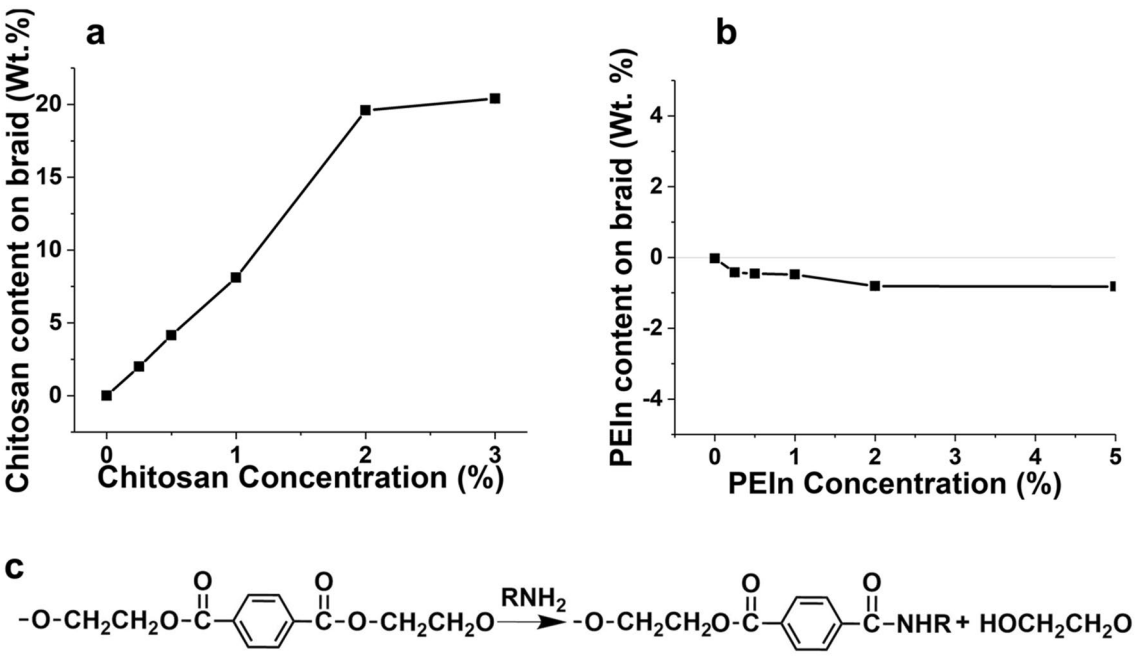

Fig. 2 **a** Change in weight of the polyester braid as a function of Chitosan concentration. **b** Change in weight of the polyester braid as a function of PEIn concentration. **c** The reaction of the amine group in the PEIn with the ester group of polyester fiber

chitosan surface-adsorbed chitosan polymer can be observed in Fig. 3b, which increased with the increase in concentration. On the contrary, no observable morphological changes were seen on the polyester structures before and after PEIn-functionalization, as determined by the SEM analysis in Fig. 3c. However, in a previous finding by Bech et al., a reduction in the diameter of the PEIn-modified polyester fiber was observed during SEM analysis and attributed due to the chemical etching of the polyester surface with PEIn (Bech et al. 2007).

The surface-modified braided structures were further investigated by ATR-FTIR, Fig. 3d, e. The powdered-chitosan (red line) spectrum shows a broad band at 3500–3000 cm^{-1} due to the –O–H and –N–H stretching vibrations. The black-lined spectrum of the control polyester braid with a characteristic ester-carbonyl peak at 1721 cm^{-1} shows no –N–H stretching at 3500–300 cm^{-1}. However, in a blue-lined spectrum of the chitosan-functionalized polyester braid, the appearance of both –O–H and –N–H stretching at 3500–3000 cm^{-1} and characteristic ester-carbonyl peak at 1721 cm^{-1} can be observed, which is attributed to the molecular interaction between protonated chitosan and polyester fibers, Fig. 3d. Analogous to SEM analysis, no significant molecular changes were detected by FTIR analysis in the polyester braided structure before and after coating with PEIn solution. The PEIn solution (black line) spectrum shows a PEIn characteristic broadband at 3288 cm^{-1} due to the due to –N–H stretching. However, both in the red line spectrum of the control polyester braid and blue line spectrum of PEIn-functionalized polyester braid, no –N–H stretching vibrations were observed between 3200 and 3300 cm^{-1}, Fig. 3e.

3.2 Effect of functionalization on EOF

Polyester threads and yarns have been reported as ideal substrates for capillary zone electrophoresis due to their highly negative zeta-potential and fast cathodic EOF at pH 8 and above (Narahari et al. 2015; Khan et al. 2020; Wei and Lin 2016; Wei et al. 2013; Quero et al. December 2018). Adsorption of positively charged chitosan on the surface of negatively charged polyester fibers will change the surface's zeta-potential, which in turn modifies the EOF. Different chitosan concentrations were used to investigate the change in EOF mobility on the surface of textile structures at pH 8. A significant decrease in EOF was observed with the lowest tested concentration of chitosan (0.25% in solution), indicating the modification of the interfacial double layer due to chitosan adsorption on polyester, Fig. 4a.

The EOF was suppressed further as the chitosan concentration increased by the adsorption of more chitosan molecules on the surface. The chitosan molecules were neutral at basic pH 8 and resulted in reduced negative zeta-potential at the surface of polyester fiber. In contrast, the EOF increased and reversed its direction at pH ≤ 5 on the chitosan-functionalized braid's surface. This behavior is attributed to the presence of amino groups (pKa = 6.3) at the surface that changed the initial cathodic to anodic EOF. The EOF

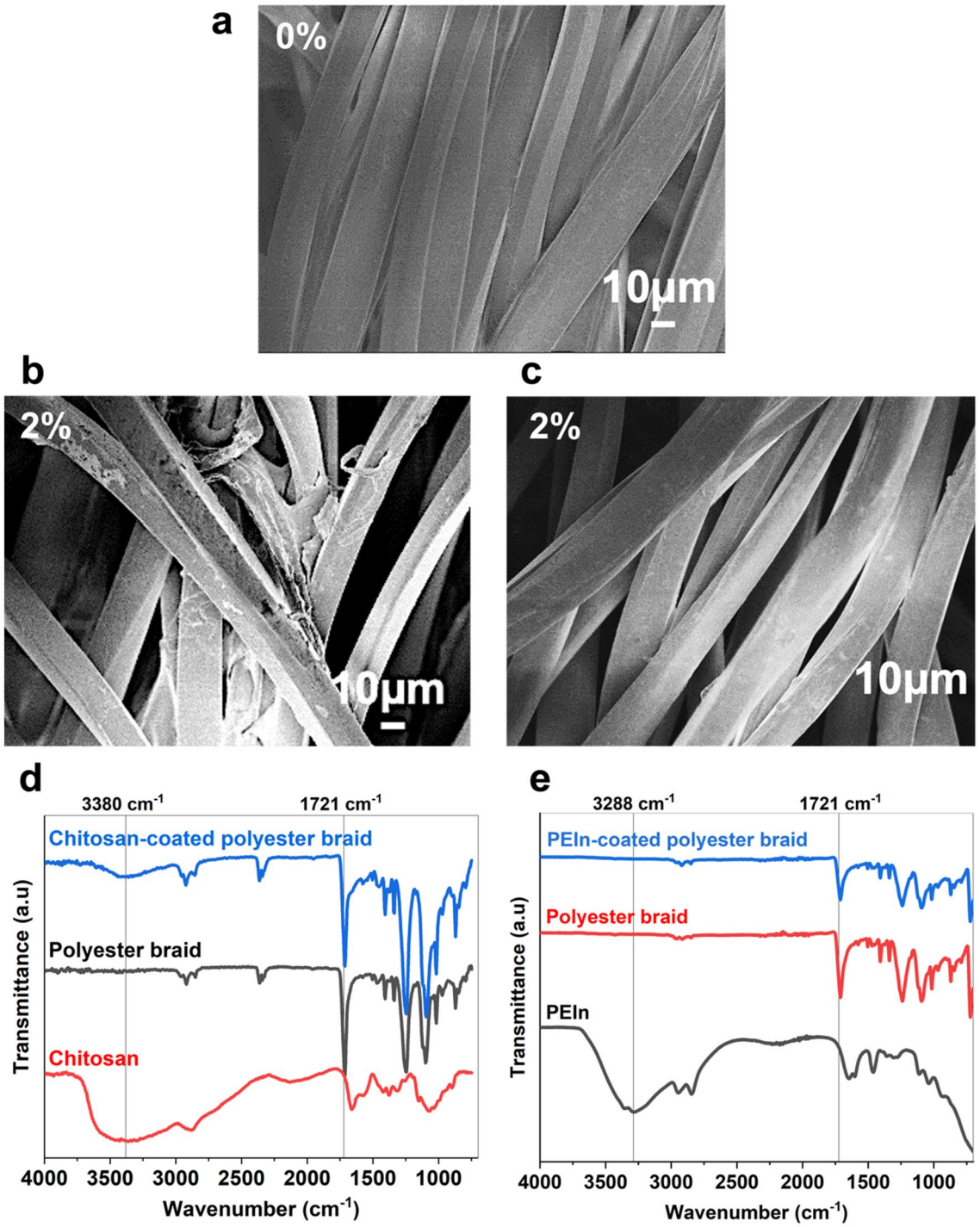

Fig. 3 Characterization of functionalized polyester braided structure. **a** SEM images of the polyester braided structure **a** before and after **b** 2% solution concentration of chitosan-functionalization and **c** 2% solution concentration of PEIn-functionalization. All micrographs were obtained at 600×. **d** FTIR-spectra of the chitosan-functionalized polyester braid (*blue*) controlled polyester braid (*black*) and pure chitosan power (*red*). **e** FTIR-spectra of the PEIn-functionalized polyester braid (*blue*) controlled polyester braid (*red*) and PEIn aqueous solution (*black*) (colour figure online)

remains relatively constant on further increase in chitosan concentrations beyond 2%, which indicates the saturation of chitosan molecules on the surface of the polyester braid at this concentration. Therefore, the braided structure coated with 2% chitosan solution was chosen for further analysis.

The high number of amino groups in branched PEIn polymer is expected to change the zeta-potential of the

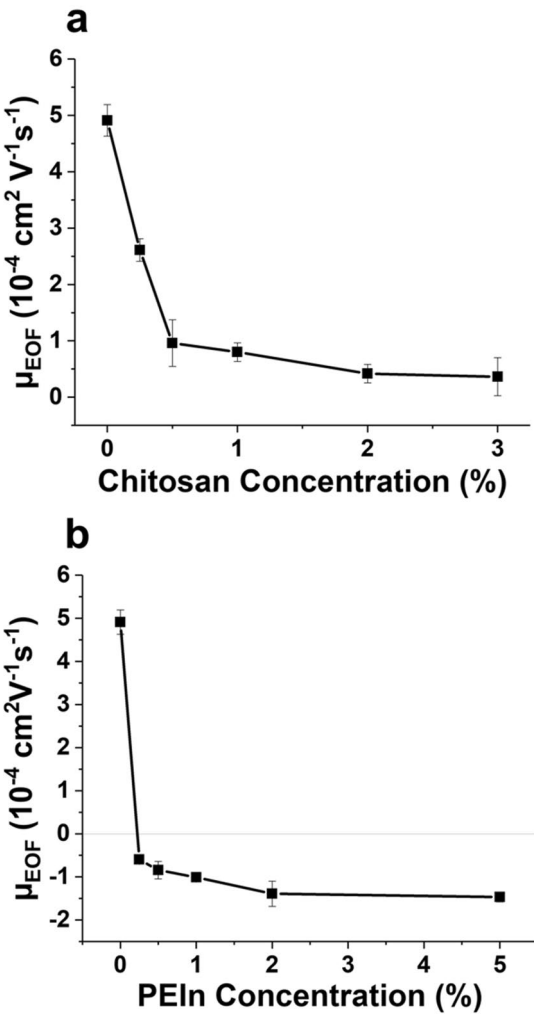

Fig. 4 **a** EOF as a function of chitosan concentration on the polyester braided structure at pH 8 with 2.5 mM TRIS/CHES buffer solution. **b** EOF as a function of PEIn concentration on the polyester braided structure at pH 8 with 2.5 mM TRIS/CHES buffer solution. Channel length, 3.6 cm; electric field 100 Vcm^{-1} and the error bare represents four EOF measurements for both (**a**) and (**b**)

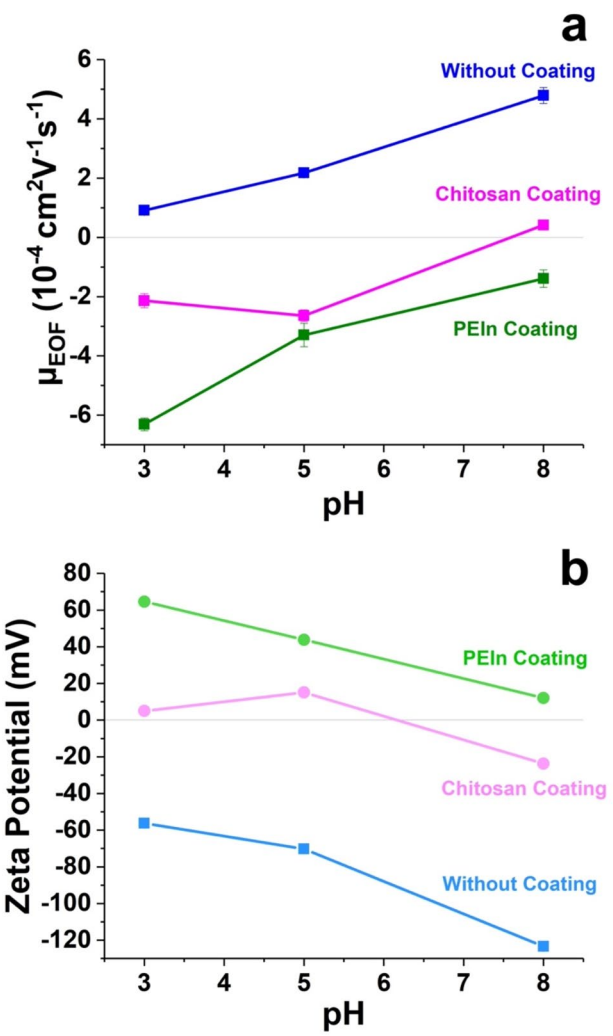

Fig. 5 Effect of functionalization on EOF. **a** EOF as a function of pH using unfunctionalized polyester braid (*blue*), functionalized with 2% chitosan solution (*pink*) and 2% PEIn solution (*green*) at 100Vcm^{-1} of electric field with channel 3.6 cm; buffers: TRIS/CHES (pH 8), Acetate buffer (pH 5), citrate buffer (pH 3), each in 3 mM concentration. **b** ζ-potential as a function of pH using uncoated polyester (*blue*), chitosan-functionalized (*pink*) and PEIn-functionalized (*green*) polyester braided structure at pH 3, 5, and 8, 1 mM KCl electrolyte solution, HCl and NaOH used for pH adjustment (color figure online)

polyester fibers, which can help in manipulating the EOF. The EOF mobility was investigated on the polyester braided structure functionalized with different PEIn polymer concentrations at pH 8. A slight reversal in the direction of EOF (from cathodic to anodic) and significant suppression of EOF was observed at the lowest tested concentration of PEIn solution (0.25%), Fig. 4b. This slight reversal of EOF was indicative of the modulation of the electric double layer at the surface of the polyester braid. However, no significant change in EOF was observed with the increase in the concentration of PEIn solution above 2%. It is also evident from the small error bars in Fig. 4 that despite the randomly oriented nature of fibers and nonhomogeneous spread of polycationic polymers on the fiber surface as indicated in the SEM images, the electroosmotic flow mobility was very consistent and reproduceable.

3.3 Effect of pH on EOF

In capillary electrophoresis, a change in pH of the background electrolyte significantly affects the EOF by altering the surface zeta-potential. EOF mobility on the control polyester braid and the chitosan—functionalized polyester braid was compared at pH 3, 5, and 8 using citrate, acetate, and TRIS/CHES buffers, respectively, Fig. 5a (pink). For

uncoated polyester fibers, the EOF direction was noted to be from the anode to cathode and its magnitude decreased with a decrease in pH. This trend was directly related to the observed reduction in the negative zeta potential of the polyester, Fig. 5a (blue). However, after chitosan functionalization, the EOF was observed to increase and reversed its direction as the pH changed from 8 to 5 due to a change in surface zeta-potential from negative to positive of the chitosan-functionalized polyester, as shown by the pink-lines in Fig. 5a, b. At pH 3, the direction of the EOF on chitosan-functionalized polyester remained anodic. However, the magnitude of EOF slightly decreased due to a decrease in the positive charge at the surface. Nevertheless, the EOF was still greater than the EOF on the unmodified polyester at the same pH. Further, the effect of pH on the EOF mobility of PEIn-functionalized braid can be observed by comparing the EOF with the control polyester at pH 3, 5, and 8, Fig. 5a (green). Here, the EOF was completely modified after treatment with PEIn in terms of both direction and magnitude with respect to the control polyester.

Before coating, the polyester braided structures show the highest EOF at pH 8, with the EOF decreasing towards acidic pH ranges of 5 and 3. For the PEIn—functionalized polyester braid, the EOF was reversed with the lowest EOF was observed at pH 8 and increasing with a decrease in pH, with the highest EOF was observed at pH 3. This behavior was consistent with the lower PEIn pKa of 4.3, which would maximize the cationic nature of the modified substrate. This trend was directly correlated with the change in the zeta-potential from negative for control polyester to positive for the PEIn-functionalized braid where the substrate was clearly cationic at all pH test values, Fig. 5b (green). Moreover, a significant suppression in the magnitude of EOF was observed at pH 8, where the EOF mobility changed from c.a. 5 to 0.5 (10^{-4} cm^2V^{-1} s^{-1}), Fig. 5b (blue – green). This significant reduction in EOF is attributed to the drastic change in zeta-potential of the polyester surface with PEIn—functionalization, which was observed as nearly zero to slightly positive. However, for the chitosan—coating, the highest EOF was observed at pH 5 with no reversal in direction at pH 8. Importantly, from these findings, it was apparent that via a simple dip—coating route, it is possible to control and manipulate both the direction and magnitude of the EOF using low-cost surface-accessible textile structures for various applications.

3.4 Effect of surface functionalization on electrophoretic separation

Electrophoretic separation of the two fluorescent markers FL and Rh-B was performed to investigate the effect of chitosan and PEIn surface functionalization of the polyester braided structures. The sample mixture (FL/Rh-B) was micropipetted (0.5 µL) at a position 1 cm from the cathodic reservoir onto the 3.6 cm long buffer-prewetted polyester braided structure, and a potential of 360 V was applied to driving electrodes. The same procedure was repeated with a chitosan and PEIn functionalized braids, and the movement of two fluorescent solutes was monitored against time, Fig. 6. In the case of uncoated polyester braid, at pH 8, for both solutes, the negatively charged FL and neutral Rh-B migrated towards the cathode under the influence of strong cathodic EOF, Fig. 6a and can be seen in video V1 in supporting information S4. The anionic FL also experienced the competing electrokinetic force towards the anode in a counter-EOF direction resulting in a smaller migration velocity than the neutral Rh-B, which flowed with the direction of the EOF.

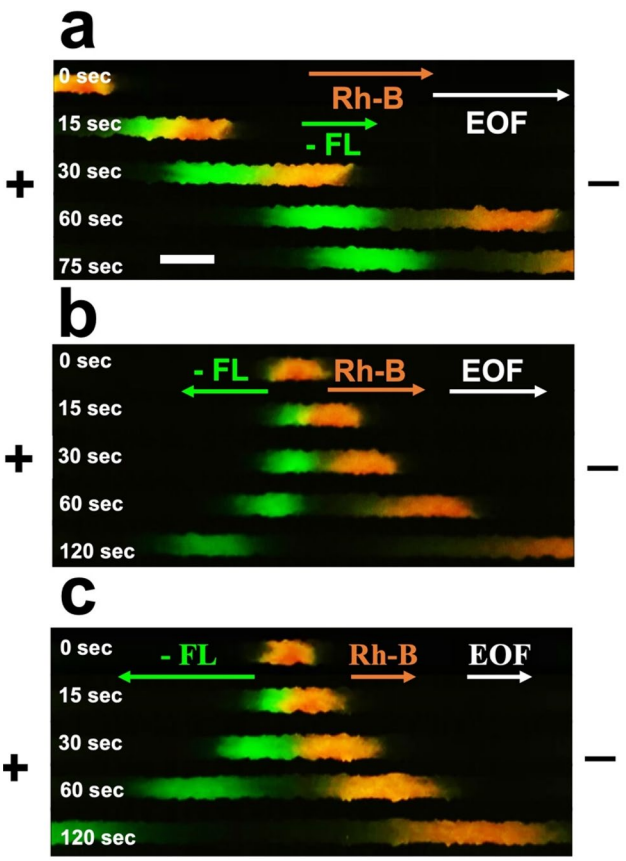

Fig. 6 Effect of functionalization on electrophoretic separation. **a** Images showing the electrophoretic separation of anionic FL (*green*) and zwitterionic Rh-B (*orange*) on a controlled polyester braided structure. **b** Electrophoretic separation on a chitosan-functionalized polyester braided structure. **c** Electrophoretic separation on a PEIn-functionalized polyester braided structure. Channel length 3.6 cm, 100Vcm^{-1} of Electric field; 2.5 mM TRIS/CHES as background electrolyte; Sample mixture consisted of FL and Rh-B in molar concentration 0.07 mM and 4 mM, respectively. Scale bar 2 mm for all frames on (**a**) (**b**) and (**c**) (color figure online)

The FL and Rh-B appeared to completely separate over 75 s, forming broad bands. Due to the high porosity of the controlled polyester braid, the broad solute bands could be ascribed to the adsorption and diffusion of solutes due to higher solute fiber interaction. For the chitosan-functionalized polyester braid, upon applying the same electric field, the anionic FL moved towards the anode while the Rh-B moved towards the cathode, as evident by the video V 2 in supporting information S 3. This change was due to the significant suppression of EOF at pH 8. As a result, the chitosan-polyester surface zeta-potential being weakly negative, Fig. 5 (b, pink), resulting in a shift towards charge-dependent electrophoretic mobility of the solutes dominating the direction of ion movement, Fig. 6b. Moreover, the separation time was also reduced with the two solutes separating completely after 60 s, forming two distinct and less diffused bands due to the counter directional solute movement.

The effect of PEIn surface-functionalization on the electrophoretic separation was monitored following the same protocols used for chitosan analysis. For the PEIn-functionalized braid, due to the suppression of the EOF at pH 8, the negatively charged FL migrated towards the positive anode. The Rh-B being neutral at pH 8, moved along with the EOF towards the cathode. However, the Rh-B mobility lagged behind FL due to highly suppressed EOF at this pH level, Fig. 6c and video V5 in supporting information S4. Moreover, with the nearly zero counterflow (cathodic EOF), the FL migration was notably accelerated on PEIn-functionalized braid in the anodic direction. Contrasting this observation, using both the control polyester braid and chitosan-functionalized braid, the FL moved slower than the Rh-B due to opposing cathodic EOF at pH 8, which provided a retarding mobility force. Therefore, it is clear that different cationic coatings affected the electrophoretic separation differently, and these differences may be beneficial for the selective separation of different analytes in a multiplex assay.

3.5 Effect of surface functionalization on ITP

The band broadening and sample diffusion was further minimized and eliminated using an ITP approach. ITP is a well-known technique for the preconcentration and focusing of broad and diffuse analyte band (Smejkal et al. 2013). In the ITP, sample solutes are concentrated between the two discontinuous electrolyte systems with anions having differential electrophoretic mobilities that are either higher and lower than the mobility of the anionic solute of interest. By using a common counter-cation in both electrolyte systems, the leading electrolyte (LE) will have higher mobility than the trailing electrolyte (TE). The TE with lower mobility (and higher resistivity) results in a higher electrical field within the TE, which then drives and enhances the overall EOF with respect to the LE. Consequently, the solute anion with an intermediate mobility will effectively be sandwiched between the TE and LE boundary to form a discretely concentrated band.

Here, we demonstrated the effect of chitosan and PEIn surface functionalization on ITP focusing and separation of an anionic FL from a mixture containing Rh-B and comparing the ITP behavior to a control polyester braid, Fig. 7. For the unmodified polyester braid, FL separated from Rh-B mixture within first 30 s and migrated towards cathode due to dominant cathodic EOF. With Rh-B being chargeless at pH 8, it migrated unimpeded under the influence of the EOF into the cathodic reservoir. However, as the FL migrated along the braid channel, the initial band broadening observed due to diffusion and solute-fiber interactions was reversed upon reaching the boundary between LE and TE ions, resulting in a focusing of the FL after 120 s, Fig. 7a\. In this instance, the FL band eventually eluted into the cathodic reservoir without achieving complete focusing due to the high EOF. This effect could be avoided by increasing the channel length but at the cost of a longer analysis time. This behavior can be more clearly observed in video V 3 in supporting information S 3. Contracting this behavior on the chitosan-functionalized braid, FL was focused and enriched within 30 s. The enriched FL band then migrated towards the oppositely charged anode forming a sharp and enriched focused band after 120 s, which was maintained until it reached the edge of the anodic reservoir. With the EOF suppressed, the chargeless Rh-B remained broad and essentially static after 120 s. These ITP findings clearly suggest that the chitosan surface functionalization of polyester, modulated the EOF, significantly enhanced the separation efficiency, and created a sharp enriched analyte band, as evident in Fig. 7b and video V 4 in supporting information S 3.

ITP sample staking and separation of FL from the mixture was also monitored on the PEIn-functionalized braids, Fig. 7c. The FL was successfully separated from the mixture and focused into an enriched band at 120 s. After FL focusing, the neutral Rh-B remained relatively static, indicating an effective suppression of the EOF. However, some degree of diffusion broadening can be seen in Fig. 7c and video V 6 in S4, which is likely due to the solute-fiber interactions. It is apparent that a more resolved and narrower peak was obtained with chitosan-functionalized braid when compared to the control and PEIn-functionalized braids, Fig. 6. However, for the PEIn-functionalized system, due to the suppression of the cathodic EOF to nearly zero EOF, at the basic pH, a fast movement of FL was observed, where the FL migrated to the end of the anodic edge of the braid within 130 s (Fig. 7c compared to chitosan-functionalized braid where FL traveled the same distance over 180 s (Fig. 7b. Contrasting this finding, the control polyester channel with the highest cathodic EOF at a basic pH resulted in the migration of the

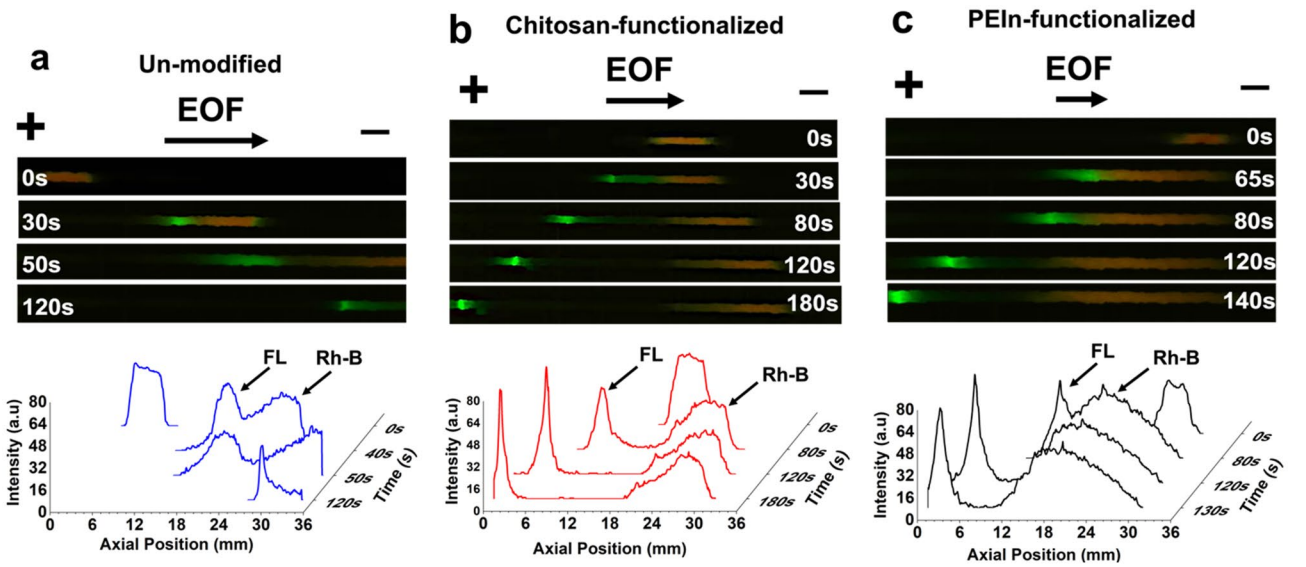

Fig. 7 Effect of functionalization on ITP sample staking. **a** Fluorescence and extracted gray-scale intensity profile of ITP separation and concentration of FL and Rh-B using a control polyester braid. **b** Fluorescence and extracted gray-scale intensity profile of ITP separation and concentration of FL and Rh-B using chitosan-functionalized polyester braid. **c** Fluorescence and extracted gray-scale intensity profile of ITP separation and concentration of FL and Rh-B using PEIn-functionalized polyester braid. ITP was performed using 3.6 cm long channel length; 20 µA of constant current; LE: 2.5 mM TRIS + 100 mM HCl and TE: 2.5 mM of TRIS and 25 mM of HEPES; FL-Rh-B sample mixture was prepared in TE in a molar ratio of 0.07 mM:4 mM, respectively

solute into the cathodic reservoir without achieving focusing or separation, Fig. 7a. This simple approach demonstrates the selective flow dynamics can be imparted onto the textile structures for analytical applications which can manipulate, redirect, extract, and enrich charged analytes.

4 Conclusion

In conclusion, a versatile and nascent method has been introduced to significantly improve the electrophoretic properties of textile-based microfluidics with the help of a simple surface adsorption modification. Two types of cationic polymers, chitosan and PEIn, were used for the surface modification of polyester braided structures via a simple dip-coating approach. It is shown that surface functionalization of textiles with chitosan and PEIn fundamentally alters the EOF and electrophoretic mobilities of the charged solutes in terms of magnitude and direction when tested over a range of pH. The two types of coatings were compared to determine their influence on EOF, and electrophoretic separation of two solutes (anionic FL and zwitterionic Rh-B). Additionally, the ability to simultaneously separate and focus the anionic FL from Rb-B was demonstrated using an isotachophoretic (ITP) focusing approach. The chitosan-surface functionalization of polyester structures resulted in a suppression of the EOF at basic pH and reversal in the direction of EOF at acidic pH. However, the PEIn-surface functionalization on polyester was shown to suppress the EOF to a nearly zero level at basic pH and reversed to an anodic direction at acidic pH. EOF is generally always very slow at acidic pH < 3.5 and very fast at basic pH. Here, the PEIn-surface functionalization was observed to significantly increase the magnitude of the EOF at pH < 3.5, which is a promising finding which could facilitate fast analysis of basic analytes, especially for those with pKa < 3.5.

In terms of electrophoretic separation and ITP enrichment, the chitosan-functionalization was identified as the best route for efficient separation and ITP enrichment with good stability when compared with PEIn. The approach demonstrated here suggests that the surface functionality can be selectively tailored on low-cost textile substrates based on the targeted analytes for point-of-care analysis and other analytical applications. A key finding here is that functionality can be readily imparted upon any available low-cost textile yarns irrespective of the fiber's underlying nature. For example, using plasma functionalization, the polyethylene and polypropylene fiber's uncharged surfaces can be activated for electrophoretic analysis and immobilization of biomolecules on the surface. Similarly, direct chemical grafting of the functional groups into the textile structure could be another possible route for adopting the selective functionality on low-cost textile microfluidics.

Supplementary Information The online version contains supplementary material available at https://doi.org/10.1007/s10404-022-02603-6.

Acknowledgements The authors would like to thank the Higher Education Commission Pakistan (HEC) for Ph.D. funding and the NCRIS-enabled Australian National Fabrication Facility—Materials Node and Queensland Node for access to fabrication equipment and zeta potential measurements, respectively. Funding from the Australian Research Council (ARC) Centre of Excellence for Electromaterials Science (CE140100012) and ARC Discovery Project (DP170102572) is gratefully acknowledged.

Author contributions The manuscript was written through the contributions of all authors. All authors have given approval for the final version of the manuscript. These authors contributed equally.

Funding Open Access funding enabled and organized by CAUL and its Member Institutions.

Declarations

Conflict of interest The authors declare no conflict of interest.

References

AsadiMiankafshe M, Bashir T, Persson NK (2019) The role and importance of surface modification of polyester fabrics by chitosan and hexadecylpyridinium chloride for the electrical and electro-thermal performance of graphene-modified smart textiles. New J Chem 43(17):6643–6658

Bagherbaigi S, Córcoles EP, Wicaksono DHB (2014) Cotton fabric as an immobilization matrix for low-cost and quick colorimetric enzyme-linked immunosorbent assay (ELISA). Anal Methods 6(18):7175–7180

Baysal G, Onder S, Gocek I, Trabzon L, Kızıl H, Kok FN, Kayaoğlu BK (2014) Microfluidic device on a nonwoven fabric: a potential biosensor for lactate detection. Text Res J 84(16):1729–1741

Bech L, Meylheuc T, Lepoittevin B, Roger P (2007) Chemical surface modification of poly(ethylene terephthalate) fibers by aminolysis and grafting of carbohydrates. J Polym Sci Part A Polym Chem 45(4):2172–2183

Bendak A, El-Marsafi S (1991) Effects of chemical modifications on polyester fibres. J Islam Acad Sci 4(4):275–284

Bhandari P, Narahari T, Dendukuri D (2011) Fab-chips': a versatile, fabric-based platform for low-cost, rapid and multiplexed diagnostics. Lab Chip 11(15):2493

Boonyakong C, Tucker SA (2009) Capillary electrophoresis using core-based hyperbranched polyethyleneimine (CHPEI) static-coated capillaries. J Sep Sci 32(20):3489–3496

Bush DR, Zang L, Belov AM, Ivanov AR, Karger BL (2016) High resolution CZE-MS quantitative characterization of intact biopharmaceutical proteins: proteoforms of interferon-B1. Anal Chem 88(2):1138–1146

Cabot JM, Macdonald NP, Phung SC, Breadmore MC, Paull B (2016) Fibre-based electrofluidics on low cost versatile 3D printed platforms for solute delivery, separations and diagnostics; from small molecules to intact cells. Analyst 141(23):6422–6431

Caetano FR, Carneiro EA, Agustini D, Figueiredo-Filho LCS, Banks CE, Bergamini MF, Marcolino-Junior LH (2018) Combination of electrochemical biosensor and textile threads: a microfluidic device for phenol determination in tap water. Biosens Bioelectron 99:382–388

Chen L, Cabot JM, Rodriguez ES, Ghiasvand A, Innis PC, Paull B (2020) Thread-based isoelectric focusing coupled with desorption electrospray ionization mass spectrometry. Analyst 145:6928

Choi JR, Nilghaz A, Chen L, Chou KC, Lu X (2018) Modification of thread-based microfluidic device with polysiloxanes for the development of a sensitive and selective immunoassay. Sensors Actuators B Chem 260:1043–1051

Córdova E, Gao J, Whitesides GM (1997) Noncovalent polycationic coatings for capillaries in capillary electrophoresis of proteins. Anal Chem 69(7):1370–1379

Enescu D (2008) Use of chitosan in surface modification of textile materials. Rom Biotechnol Lett 13(6):4037–4048

Erenas MM, De Orbe-Payá I, Capitan-Vallvey LF (2016) Surface modified thread-based microfluidic analytical device for selective potassium analysis. Anal Chem 88(10):5331–5337

Fixe F, Dufva M, Telleman P, Christensen CB (2004) Functionalization of poly(methyl methacrylate) (PMMA) as a substrate for DNA microarrays. Nucleic Acids Res 32(1):1–8

Fu X, Huang L, Gao F, Li W, Pang N, Zhai M, Liu H, Wu M (2007) Carboxymethyl chitosan-coated capillary and its application in CE of proteins. Electrophoresis 28(12):1958–1963

Fu X, Liu H, Liu Y, Liu Y (2013) Application of chitosan and its derivatives in analytical chemistry: a mini-review. J Carbohydr Chem 32(8–9):463–474

Guan W, Zhang C, Liu F, Liu M (2015) Chemiluminescence detection for microfluidic cloth-based analytical devices (MCADs). Biosens Bioelectron 72:114–120

Hajba L, Guttman A (2017) Recent advances in column coatings for capillary electrophoresis of proteins. TrAC - Trends Anal Chem 90:38–44

Horvath J, Dolník V (2001) Polymer wall coatings for capillary electrophoresis. Electrophoresis 22(4):644–655

Huang X, Gordon MJ, Zare RN (1988) Current-monitoring method for measuring the electroosmotic flow rate in capillary zone electrophoresis. Anal Chem 60(17):1837–1838

Jun BM, Nguyen TPN, Ahn SH, Kim IC, Kwon YN (2015) The application of polyethyleneimine draw solution in a combined forward osmosis/nanofiltration system. J Appl Polym Sci 132(27):1–9

Khan JU, Sayyar S, Paull B, Innis PC (2020) Novel approach toward electrofluidic substrates utilizing textile-based braided structure. ACS Appl Mater Interfaces 12(40):45618–45628

Khan JU, Ruland A, Sayyar S, Paull B, Chen J, Innis PC (2021) Wireless bipolar electrode-based textile electrofluidics: towards novel micro-total-analysis systems. Lab Chip 21:3979

Kilonzo P, Margaritis A, Bergougnou M (2011) Effects of surface treatment and process parameters on immobilization of recombinant yeast cells by adsorption to fibrous matrices. Bioresour Technol 102(4):3662–3672

Kung CT, Hou CY, Wang YN, Fu LM (2019) Microfluidic paper-based analytical devices for environmental analysis of soil, air, ecology and river water. Sens Actuators, B Chem 301(April):126855

Li X, Tian J, Shen W (2010) Thread as a versatile material for low-cost microfluidic diagnostics. ACS Appl Mater Interfaces 2(1):1–6

Li YD, Li WY, Chai HH, Fang C, Kang YJ, Li CM, Yu L (2018) Chitosan functionalization to prolong stable hydrophilicity of cotton thread for thread-based analytical device application. Cellulose 25(8):4831–4840

Liang RP, Gan GH, Qiu JD (2008) Surface modification of poly(dimethylsiloxane) microfluidic devices and its application in simultaneous analysis of uric acid and ascorbic acid in human urine. J Sep Sci 31(15):2860–2867

Lucy CA, MacDonald AM, Gulcev MD (2008) Non-covalent capillary coatings for protein separations in capillary electrophoresis. J Chromatogr A 1184(1–2):81–105

Lungu CN, Diudea MV, Putz MV, Grudziński IP (2016) Linear and branched PEIs (polyethylenimines) and their property space. Int J Mol Sci 17(4):555

Martinez AW, Phillips ST, Butte MJ, Whitesides GM (2007) Patterned paper as a platform for inexpensive, low-volume, portable bioassays. Angew Chemie—Int Ed 46(8):1318–1320

Narahari T, Dendukuri D, Murthy SK (2015) Tunable electrophoretic separations using a scalable, fabric-based platform. Anal Chem 87(4):2480–2487

Owens TL, Leisen J, Beckham HW, Breedveld V (2011) Control of microfluidic flow in amphiphilic fabrics. ACS Appl Mater Interfaces 3(10):3796–3803

Quero RF, Bressan LP, da Silva JAF, de Jesus DP (2018) A novel thread-based microfluidic device for capillary electrophoresis with capacitively coupled contactless conductivity detection. Sens Actuators, B Chem 2019(286):301–305

Ragab MAA, El-Kimary EI (2020) Recent advances and applications of microfluidic capillary electrophoresis: a comprehensive review (2017–mid 2019). Crit Rev Anal Chem 51:1–33

Ratajczak K, Stobiecka M (2019) High-performance modified cellulose paper-based biosensors for medical diagnostics and early cancer screening: a concise review. Carbohydr Polym 2020(229):115463

Reches M, Mirica KA, Dasgupta R, Dickey MD, Butte MJ, Whitesides GM (2010) Thread as a matrix for biomedical assays. ACS Appl Mater Interfaces 2(6):1722–1728

Smejkal P, Bottenus D, Breadmore MC, Guijt RM, Ivory CF, Foret F, Macka M (2013) Microfluidic isotachophoresis: a review. Electrophoresis 34(11):1493–1509. https://doi.org/10.1021/ac00168a040

Stutz H (2009) Protein attachment onto silica surfaces—a survey of molecular fundamentals, resulting effects and novel preventive strategies in CE. Electrophoresis 30(12):2032–2061

Sun P, Landman A, Hartwick RA (1994) Chitosan coated capillary with reversed electroosmotic flow in capillary electrophoresis for the separation of basic drugs and proteins. J Microcolumn Sep 6(4):403–407

Sun P, Landman A, Hartwick RA (2016) Novel cationic polyelectrolyte coatings for capillary electrophoresis. Electrophoresis 37(2):363–371

Takayanagi T, Motomizu S (2006) Chitosan as cationic polyelectrolyte for the modification of electroosmotic flow and its utilization for the separation of inorganic anions by capillary zone electrophoresis. Anal Sci 22(9):1241–1244

Towns JK, Regnier FE (1990) Polyethyleneimine-bonded phases in the separation of proteins by capillary electrophoresis. J Chromatogr A 516(1):69–78

Ulum MF, Maylina L, Noviana D, Wicaksono DHB (2016) EDTA-treated cotton-thread microfluidic device used for one-step whole blood plasma separation and assay. Lab Chip 16(8):1492–1504

Walawska A, Filipowska B, Rybicki E (2003) Dyeing polyester and cotton-polyester fabrics by means of direct dyestuffs after chitosan treatment. Fibres Text East Eur 11(2):71–74

Wang S, Ge L, Song X, Yu J, Ge S, Huang J, Zeng F (2012) Paper-based chemiluminescence ELISA: lab-on-paper based on chitosan modified paper device and wax-screen-printing. Biosens Bioelectron 31(1):212–218

Wei YC, Lin CH (2016) Capillary electrophoresis and electrospray ionization on a single-thread microfluidic system for rapid mass spectrometry detection. IEEE, MEMS 25:485–488

Wei YC, Fu LM, Lin CH (2013) Electrophoresis separation and electrochemical detection on a novel thread-based microfluidic device. Microfluid Nanofluidics 14(3):583–590

Weng X, Neethirajan S (2018) Paper-based microfluidic aptasensor for food safety. J Food Saf 38(1):e12412

Weng X, Kang Y, Guo Q, Peng B, Jiang H (2019) Recent advances in thread-based microfluidics for diagnostic applications. Biosens Bioelectron 132:171–185

Whitesides GM (2006) The origins and the future of microfluidics. Nature 442(7101):368–373

Xing S, Jiang J, Pan T (2013) Interfacial microfluidic transport on micropatterned superhydrophobic textile. Lab Chip 13(2):1937–1947

Xu C, Jiang D, Lin J, Cai L (2018) Cross channel thread-based microfluidic device for separation of food dyes. J Chem Educ 95:1000–1003